Ab initio many-body Green's function calculations of optical properties of LiF at high pressures

Catalin D. Spataru, Luke Shulenburger, and Lorin X. Benedict

Phys. Rev. B **92**, 245117 — Published 10 December 2015

DOI: 10.1103/PhysRevB.92.245117

Ab initio many-body Green's function calculations of optical properties of LiF at high pressures

Catalin D. Spataru[1], Luke Shulenburger[2], and Lorin X. Benedict[3]
[1]*Sandia National Laboratories, Livermore, CA 94551, USA*
[2]*Sandia National Laboratories, Albuquerque, NM 87185, USA*
[3]*Lawrence Livermore National Laboratory, Livermore, CA 94550, USA*
(Dated: November 19, 2015)

We present Density Functional Theory (DFT) + quasiparticle self-energy (G_0W_0) + Bethe-Salpeter calculations of the real and imaginary parts of the long-wavelength dielectric function of LiF between ambient pressure and P= 5 Mbar. While the optical absorption spectrum is predicted to show dramatic pressure-dependent features above the optical gap, the index of refraction well below the gap is shown to exhibit the same trends as that seen in both DFT calculations and experiment: a roughly linear increase with density. This increase does not result from a decrease in the band gap, but rather follows from the increase in oscillator strength which counteracts a smaller increase in band gap with P. Our calculations also suggest that the index of refraction (for visible and near-UV light) of the higher-T B_2-phase should be quite close to that of the B_1 (ambient crystalline) phase. These findings may be of interest to researchers who use LiF as a window material in dynamic compression experiments.

I. INTRODUCTION

Lithium fluoride has one of the largest optical gaps (over 11 eV) of any solid at standard temperature and pressure[1]. The perfect crystalline LiF solid is therefore transparent well into the vacuum ultraviolet. As is typical for materials with large band gaps, the optical absorption spectrum for photon energies just above this gap is dominated by excitons having a large charge-transfer character. Such features in LiF have been captured very well by *ab initio* electronic structure theories which include both quasiparticle self-energy corrections and electron-hole interactions in the (assumed) singly-excited final state[2].

Since LiF has such a large optical gap, it has been used for years as a window material in dynamic compression (e.g. shock) experiments[3,4]. In such studies, pressure waves are sent into a sample, and the subsequent material response is interrogated by reflecting light off one or more of the sample's surfaces. This light often traverses a LiF window before and after hitting the sample under investigation, and thus it is essential that two features of the optical properties of LiF are known at elevated pressures: 1. The stress states for which LiF is transparent to the optical radiation (usually emanating from various lasers), and 2. The index of refraction of LiF in such states of compression, essential for knowing the total optical path length needed to correctly interpret fringes resulting from interference between reflected and un-reflected light.

Because of these applications (in addition to its fundamental interest as a prototypical wide-gap material) LiF itself has been the subject of a number of dynamic high-pressure experimental investigations[5–11]. Several of these have focused specifically on its high-pressure optical properties, and have collectively determined the real part of the index of refraction, n, for densities up to just over 4 g/cm^3 ($\sim$ 60% increase in density above ambient)[5,8–11]. In particular, Jensen et al. showed that n for two different laser wavelengths (532 nm and 1550 nm) is linearly increasing with density[8]. This was later modified by Rigg et al[11], who performed more measurements along the shock Hugoniot and determined quadratic corrections to this linear behavior. The work of Fratanduono et al.[10] used laser drives and ramp compression to access much larger densities (up to $\rho \sim 7$ g/cm^3, $[\rho/\rho_0] \sim 3$, P up to 8 Mbar), and inferred a linear increase of n with ρ over this whole range, consistent with the lower-compression data. From these results, Fratanduono et al. extrapolated the behavior of a simple model[12] based on the oscillator-strength sum rule to infer that the optical gap of LiF may close under hydrostatic stress at a density of ~ 11 g/cm^3.[10] This extrapolation assumed, among other things, that the increase in n results from a decrease in the optical gap, $E_{\rm gap}^{\rm opt}$, therefore implying that $E_{\rm gap}^{\rm opt}$ decreases with compression.

While $E_{\rm gap}^{\rm opt}$ is indeed known to decrease with increasing ρ for many materials, recent Density Functional Theory (DFT) calculations of crystalline LiF[13] have predicted just the opposite, at least for the ambient B_1-phase (cubic, NaCl structure). However, these calculations also show an index of refraction which increases with compression for photon energies well below $E_{\rm gap}^{\rm opt}$, in agreement with experiment. This indicates that the true relationship between n and $E_{\rm gap}^{\rm opt}$ is likely more subtle than that assumed in ref.[10], calling into question their extrapolated prediction of the ultimate compression required for optical gap closure. In addition, these recent DFT predictions of n[13] at the relevant laser wavelengths are in decent numerical agreement with the measured values in the neighborhood of ambient conditions. This is not surprising: While standard DFT fails to account for both quasiparticle self energy effects and excitonic binding, it has long been known that the index of refraction for photon energies well below $E_{\rm gap}^{\rm opt}$ is generally well predicted[14]. However, it is expected that the detailed shape of the op-

tical absorption spectrum itself (for $\hbar\omega > E_{\rm gap}^{\rm opt}$) is rather poorly predicted by DFT alone, given the aforementioned ambient-pressure theoretical studies[2].

DFT calculations of the optical properties of shocked LiF have been performed as well, some years before the recent study[13], and in response to the interest in the refractive index from the experimental community[5,6]. In that work[15,16], it was shown that DFT molecular dynamics predictions of the optical reflectivity are in reasonable agreement with experiment for the hot dense fluid (above ~ 4.5 g/cm^3 for states on the principal Hugoniot). However, it was acknowledged that the solid is improperly treated, due to the neglect of quasiparticle self-energy and excitonic effects[15,16], thereby calling into question the applicability of those predictions for the more recent ramp compression experiments[10] which are presumed to remain solid even in multi-Mbar conditions.

In this work, we perform DFT + quasiparticle self-energy + Bethe-Salpeter equation (BSE) calculations of both the optical absorption spectra and the resulting indices of refraction for crystalline LiF in conditions of high stress. The quasiparticle self energies are computed in the single-iteration GW method (G_0W_0)[17]. As in the DFT predictions[13], we find that $E_{\rm gap}^{\rm opt}$ increases with applied hydrostatic stress, but we also find that it decreases when the compression is uniaxial. While a single large excitonic peak just above $E_{\rm gap}^{\rm opt}$ is present in the ambient-pressure absorption spectrum of LiF[1,2], we predict a series of such peaks to appear as the pressure is raised to well over 1 Mbar. The behavior of n with P is shown to be very similar to that from DFT, lending further credence to the assertion that increasing n does not necessarily imply decreasing $E_{\rm gap}^{\rm opt}$ in this material. Furthermore, we show that the increase in n (at least in the ambient crystalline phase) results from the strong increase in transition dipole matrix elements which counteracts the effect of the increase in $E_{\rm gap}^{\rm opt}$. Finally, we present results for uniaxial compression in the B_1 phase, as well as predictions for the optical constants of the high-T B_2 phase[18] (though computed at $T = 0$). These predictions allow us to address scenarios of potential importance to the dynamic high-pressure community, where LiF is used as a window material in both shock and ramp-wave experiments.

Section II contains the details of our *ab initio* many-body calculations. We present results in Section III; first the quasiparticle band structures are presented as a function of applied stress, and then optical absorption spectra and indices of refraction are discussed. We conclude in Section IV.

II. *AB INITIO* MANY BODY GREEN'S FUNCTION PRESCRIPTION

We use a Green's function many-body approach to obtain the electronic and optical properties of LiF as a function of pressure. The method involves a perturbation expansion, to first order, about the screened Coulomb interaction, W_0. Quasiparticle excitations are described via the application of the G_0W_0 self-energy operator[17], which has been used to calculate quasiparticle energies and lifetimes of a variety of materials[20], including those in extreme conditions[21,22]. Similarly, excitonic properties are obtained by solving a Bethe-Salpeter equation[23]. The calculations are done in three steps following the standard procedure[19]:

i) First, we obtain the ground state properties of the system within DFT[24]; for this, we employ the Local Density Approximation (LDA). A hard, norm conserving pseudopotential with all electrons in the valence is used for lithium, with a 0.5 bohr cutoff radius for the s channel, and a 1.2 bohr cutoff radius for the p channel. The flourine pseudopotential has only the 1s electrons in the core and has 0.6 bohr cutoffs for both the s and p channels. Both pseudopotentials were generated using the OPIUM pseudopotential generation package[25]. The DFT calculations are performed with the Quantum ESPRESSO package[26]. The Kohn-Sham eigenvalues and eigenfunctions are then used to construct the one-particle Green's function, G_0. Our choice of pseudopotentials necessitated the use of a 500 Ryd plane wave energy cutoff in the description of these Kohn-Sham states.

ii) Next, we obtain the quasiparticle self-energy corrections via the G_0W_0 approximation for the electron self-energy[17]. The Brillouin zone is sampled with a Monkhorst-Pack grid of dimension $10 \times 10 \times 10$. The screened Coulomb interaction, W_0, is constructed from the irreducible polarizability via the Random Phase Approximation (RPA) using up to 500 empty bands and a 25 Ry energy cutoff for the description of the matrix elements entering the RPA expression[27]. These choices ensure, within the method used, a numerical accuracy in the quasiparticle band energies of 0.1 eV, which is sufficient for our computation of the optical properties in this work.

iii) Finally, our exciton states (assumed to be linear superpositions of single quasielectron-quasihole pairs) are constructed as solutions to the Bethe-Salpeter equation with a particle-hole interaction kernel derived from the statically screened Coulomb interaction[2,23]. These calculations consider all 5 valence bands and the lowest 10 conduction bands for each $\mathbf{k}$-point. From the calculated exciton wave functions and eigenvlaues we evaluate optical properties such as linear absorption spectra and the index of refraction, n.

Our calculations assume low temperature as appropriate for ramp-compression experiments[10], and perfect crystalline phases subjected to: i) hydrostatic pressure, P, which is expected in a dynamic experiment for stresses greater than the elastic limit. ii) uniaxial strain appropriate for much smaller stresses in the elastic regime. However, we consider such uniaxially compressed states for stresses well beyond the nominal elastic regime here; this we do to determine the optical response of LiF *before* the material has had time to relax to the hydrostat through

the creation and rearrangement of defects and dislocations, though to our knowledge this regime has not yet been probed experimentally[6].

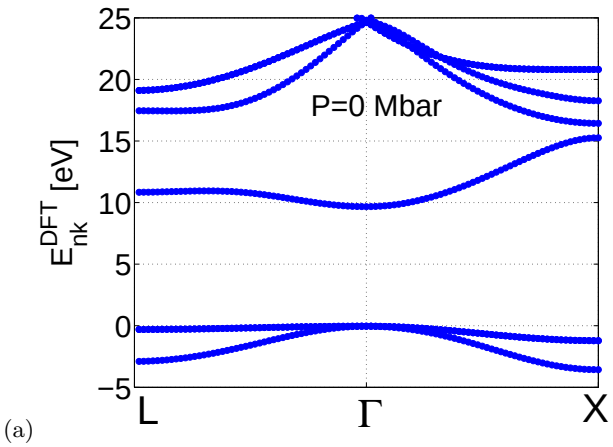

(a)

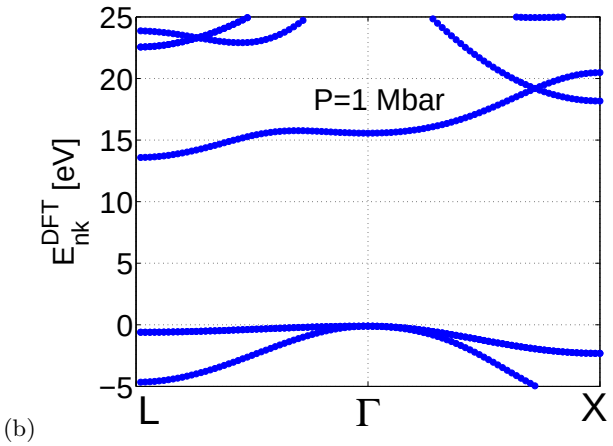

(b)

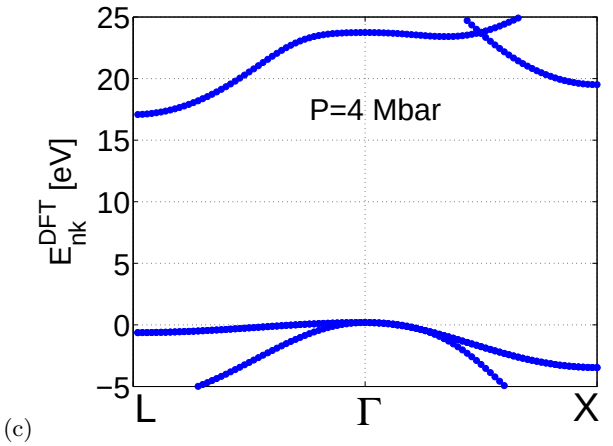

(c)

FIG. 1: Electronic bandstructure (DFT level) of LiF under hydrostatic pressure: (a) $P = 0$ Mbar. (b) $P = 1$ Mbar. (c) $P = 4$ Mbar.

III. RESULTS

A. Electronic structure and optical absorption spectra at elevated pressures

Fig 1 shows the DFT bandstructure of LiF for several P. We consider hydrostatic pressures from P=0 to 5 Mbar, which correspond to densities ranging from $\rho = 2.6$ to 6.4 g/cc, or Li-F interatomic distances ranging from $d_{Li-F} = 1.95$ to 1.45 $\AA$. We note that the band gaps increase with P, and that the minimum band gap moves from being direct ($\Gamma \rightarrow \Gamma$) at $P = 0$ to indirect ($\Gamma \rightarrow L$) near P=1 Mbar, in agreement with a previous DFT-based study[13]. We also note that the positions of the conduction states are more affected by the application of pressure than are the valence bands; in particular, conduction electrons seem to delocalize more with P than valence electrons, as evidenced by the increased bandwidth of the conduction states (not clearly shown here) upon the application of pressure.

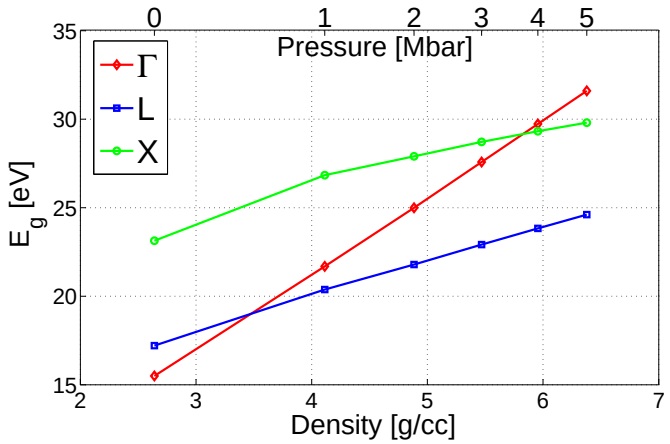

(a)

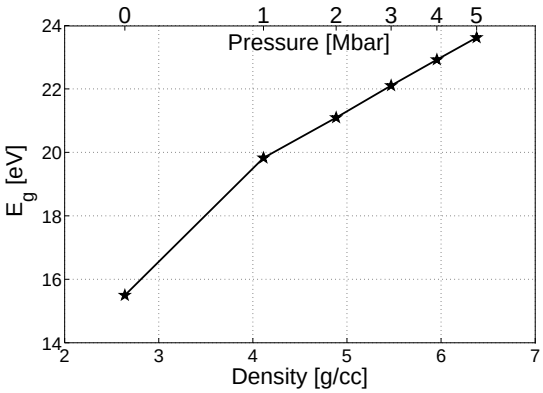

(b)

FIG. 2: Quasiparticle band gaps (G_0W_0 level) of LiF as function of hydrostatic pressure/density: (a) direct band gaps at several high-symmetry k-points. (b) minimum band gap.

The inclusion of quasiparticle self-energy corrections within the single-iteration G_0W_0 approximation leads to even larger band gaps, as traditionally found for essentially all insulating materials[28]. Fig. 2a shows the calculated QP direct gaps at L,G and X as a function of density, ρ. We note an almost linear increase with ρ, as well as a cross-over of the minimum direct gap from Γ to L as P is increased beyond 1 Mbar. Fig 2b) shows the minimum band gap, ranging from ~ 15 eV at ambient P to ~ 24 eV at $P = 5$ Mbar. This large increase with P is primarily due to the Hartree term: In LiF at ambient conditions, high-lying valence electrons are preferentially localized near F while low-lying conduction electrons reside nearer to Li. As the inter-atomic distances decrease with pressure, the "center of gravity" of the charge density corresponding to the low-lying conduction electrons moves slightly away from Li and more towards F. This is shown in fig. 3 where maximally localized Wannier functions[29] associated with the lowest conduction band are plotted at several different pressures; the big red lobe which engulfs a Li ion (yellow ball) for $P = 0$ moves away from it slightly for $P = 5$ Mbar, and the smaller lobes on adjacent F ions (light blue) increase in size as P is increased. It therefore follows that the electrostatic interaction with the ground state electron charge density increases with decreasing inter-atomic distances i) more for conduction electrons, due to Li-F first-neighbor interactions as well as interactions about a F atom, and ii) less for valence electrons, due to F-F second-neighbor interactions. We find that the p-like orbitals centered on the F ions that describe the valence band are much less dependent upon pressure.

This predicted increase of the LiF band gap with P[13] is especially interesting given the experimental results for the pressure-dependence of its optical properties. Indeed, a simple model is often used to relate the index of refraction, n, to the *average* optical gap, E_0: $n^2 = E_d E_0/(E_0^2 - \hbar^2\omega^2) + 1$, where E_d is the so-called dispersion energy and $\hbar\omega$ is the photon energy[12]. Assuming that the oscillator strength embodied in the E_d parameter is roughly constant, and assuming as well that the average gap (E_0) is proportional to the (minimum) optical gap, larger n implies a smaller gap[10]. This is in contrast to our findings for the quasiparticle band gap, at least for the lower-P, and we will see below that it will remain so for the optical gap as well once excitonic binding is included. We suggest that a simple model relating n to the optical gap is incomplete here; further work should be done at higher-P to assess the actual onset of band-gap closure in LiF.

Our predictions of optical properties, including the effects of excitons in the final state of linear absorption, are obtained via *ab initio* calculations using the statically-screened Bethe-Salpeter equation, the results of which are shown in fig. 4. Here the absorption spectra are plotted for several P. At ambient pressure, the calculated optical gap of 13.4 eV is in good agreement[30] with both experiment[1], and the results of previous calculations using similar approaches[2,31]. We note that the optical gap increases with P, due to the corresponding increase of the quasiparticle band gap. We also note a general increase in the oscillator strength of excitons with P, which we ascribe to the increasing localization of the lowest-lying conduction states away from Li and closer to F (see fig. 3) which then overlap more with the electrons in the vicinity of the F atoms, thereby increasing the conduction-valence overlap. This increased absorp-

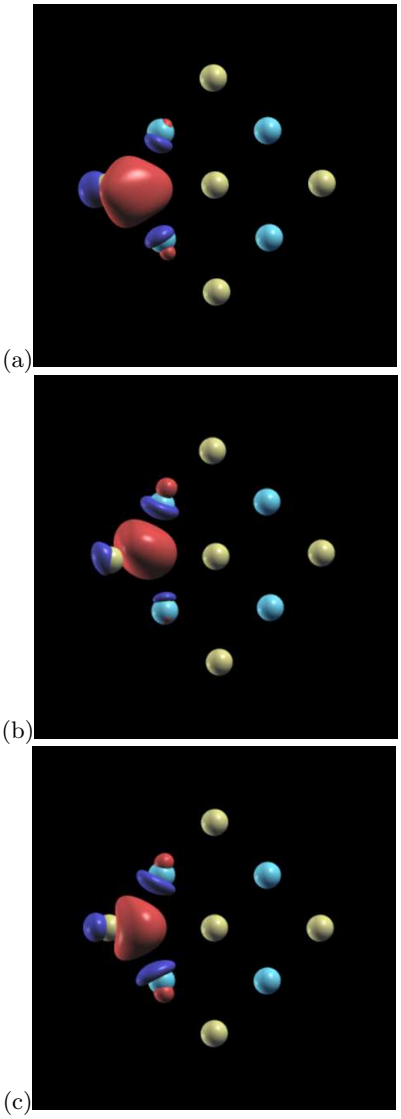

FIG. 3: Isosurface plot of the Wannier function associated with the lowest energy conduction band in LiF for several hydrostatic pressures: (a) $P = 0$ Mbar. (b) $P = 1$ Mbar. (c) $P = 5$ Mbar. For consistency the nearest distance between atoms is shown as constant although the lattice constant is decreasing with pressure as described elsewhere in the text. The yellow-colored balls represent the Li atoms while the light-blue-colored balls represent the F atoms. The red isosurface is shown at 30% of the wavefunction maximum, while the blue one is at the corresponding negative value.

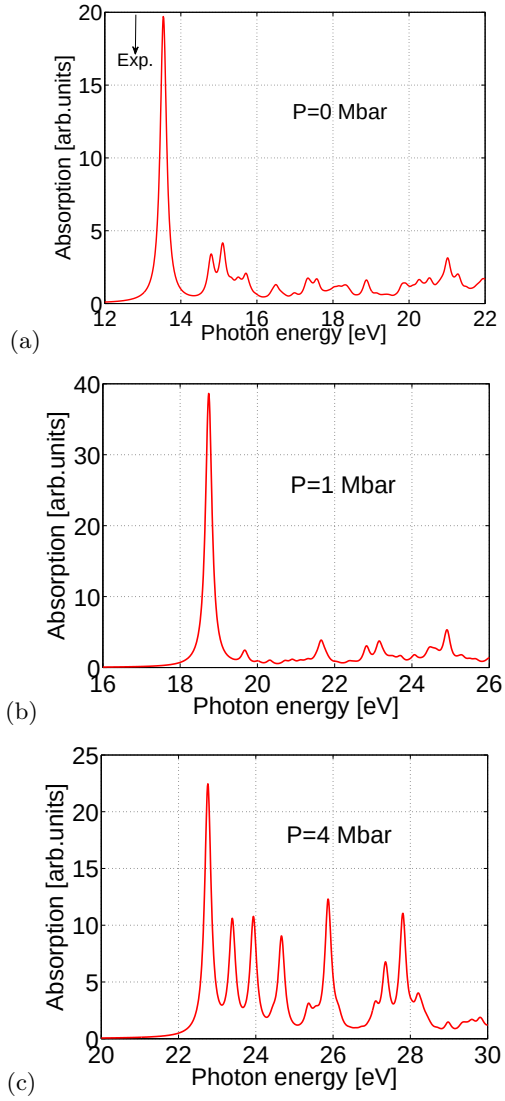

FIG. 4: Optical absorption spectra (including excitonic effects) of LiF under hydrostatic pressure: (a) $P = 0$ Mbar. (b) $P = 1$ Mbar. (c) $P = 4$ Mbar. The arrow in panel (a) indicates the experimental value of the optical gap measured at ambient pressure[1].

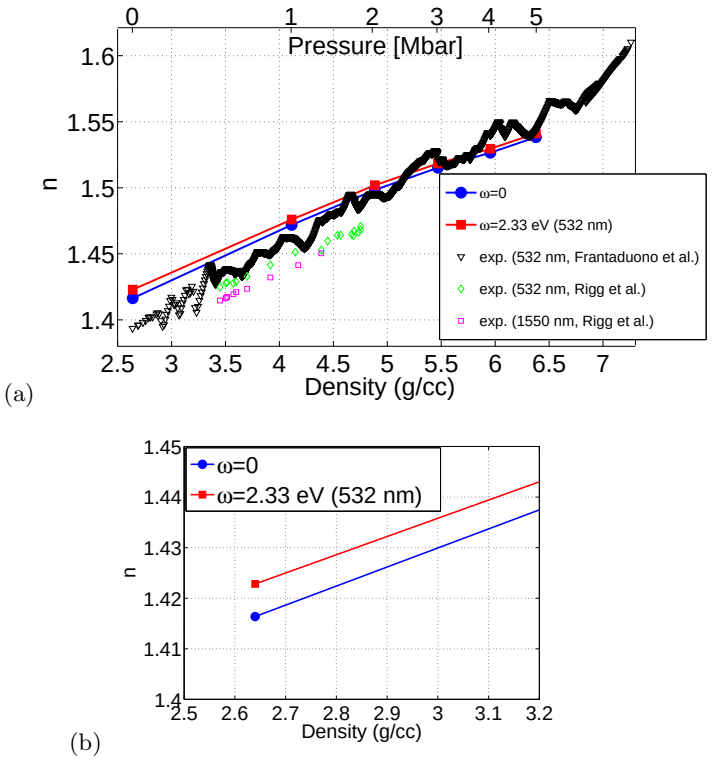

FIG. 5: (a) Index of refraction of LiF as function of hydrostatic pressure/density, calculated for two light frequencies (visible -red points- and low infrared -blue points), as well as the experimental data (ramp compression) obtained by Frandanduono et al.[10] (black points) and (shock compression) obtained by Rigg et al.[11] (green and magenta points). (b) Zoom-in of the theoretical data shown in (a).

tion just above the optical gap counteracts the increase in the gap itself, ultimately leading to an increase of n with P, as shown below. A similar set of circumstances was discussed recently in other contexts[32]. In the context of the simple model for the index of refraction[12] used in ref.[10], this results in an increase in dispersion energy (E_d) which counteracts the increase in the optical gap (E_0) with P.

Turning to the features at slightly higher photon energy, comparison between Figs. 4b and 4c shows a marked increase in the prominence of peaks in the absorption spectrum within the first 5 eV above the primary exciton feature. Such enhanced features at these same pressures are *not* apparent in our DFT-RPA spectrum, and it is therefore clear that they result from our inclusion of the electron-hole interaction in the final state of the optical absorption process. We are aware of no measurement of these features at present; indeed, such a measurement would be complicated both by the very high pressure (4 Mbar, which exceeds the highest pressures readily attainable in static high-P studies), and by the fact that the photon energy is well into the vacuum ultraviolet.

B. Index of refraction at elevated pressures: Comparisons to experiment

Fig. 5 shows the calculated real part of the index of refraction, n. We consider both $n(\omega = 0)$ and $n(\lambda = 532\text{nm})$ ($\hbar\omega = 2.33$ eV), as in recent experiments[8,11] where n was additionally determined in the infrared ($\lambda = 1550$ nm). We see that our calculated n increases almost linearly with ρ, but with a slight downward curvature. This trend is in excellent agreement with the results of the available experimental data[5,8–11], and par-

ticularly so for the recent results obtained by Rigg et al.[11], reproduced here as the green and magenta points in fig. 5a. Note, however, that our *ab initio* predictions overestimate the values of n relative to those of experiment by $1-2\%$ in the range 2.5 g/cm^3 $< \rho <$ 5 g/cm^3. While the data of Rigg et al. were taken on the shock Hugoniot of LiF rather than on a low-T isotherm as assumed by us in our calculations, we do not believe that this is the reason for the discrepancy in the magnitude. Ramp experiment results of the index of LiF[10], displayed as the black symbols in fig. 5a, show similar magnitudes in this range of density; such experiments are necessarily at somewhat lower-T for a given ρ than those of Rigg et al. Note that the ramp compression results show a slope (n vs. ρ) which is slightly larger than that of our results and those of Rigg et al. We do not currently have a clear explanation for the small discrepancies between our results and those of the experiments, though we suspect that they are in large part due to errors intrinsic to the DFT-G_0W_0-BSE prescription.

Figure 6 shows n calculated in 2 ways: including many-body (quasi-particle self-energy and excitonic) effects, and within the independent-particle picture (RPA using DFT wave functions and eigenvalues). Note that the DFT-RPA predictions of n are larger than those of DFT-G_0W_0-BSE. In this sense, we see that our inclusion of many-particle effects does seem to improve the agreement with experiment, if only slightly. More encouraging, however, is the fact that the detailed trend of the increase of n with ρ is reproduced already at the DFT-level. Since the DFT-RPA calculations are far less computationally demanding than the many-body predictions of n, this opens up the possibility of studying the role of defects, thermal disorder, and impurities on the index of refraction of LiF with large computational cells. This in turn should allow for a more detailed connection to experiment, since the regimes of interest include elevated temperatures and samples which are not likely to be defect-free, given the histories of the stress states to which LiF is typically subjected in dynamic high-pressure studies.

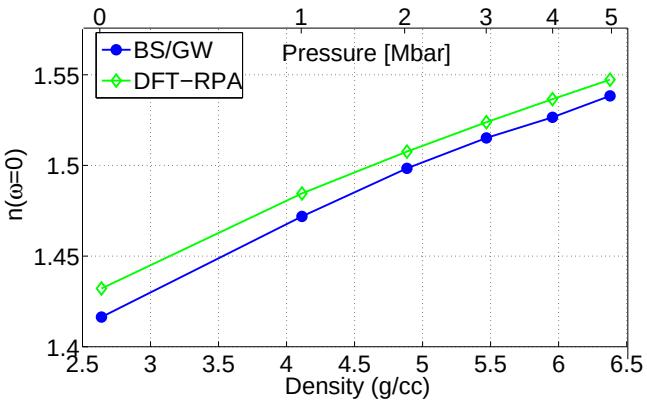

FIG. 6: Index of refraction of LiF (for light in the long wavelength limit) as function of hydrostatic pressure/density, calculated in two ways: including excitonic/quasiparticle effects at the Bethe-Salpeter-G_0W_0 level, and with no many-body effects (at the RPA level using DFT wavefunctions and eigenvalues).

C. Results for uniaxial compression

When LiF is shocked to a final stress state $\lessapprox$ 0.5 GPa (= the Hugoniot elastic limit, or HEL), it is expected to remain in the elastic regime. In the case of a single crystal, the application of a uniaxial stress will lead to a material which is uniaxially-strained along the direction of the applied stress. For final stresses $\gtrapprox$ 0.5 GPa, plastic deformation occurs to relieve the large uniaxial strain through the generation of dislocations, defects, etc. After these objects have migrated to release the local strain, a final state is reached in which, *on average*, the material is hydrostatically (or isotropically) strained rather than uniaxially strained. The precise timescale for this relaxation of local deviatoric stresses is thought to be dependent upon the final stress as well as the stress history, and for LiF, our understanding is that these timescales have yet to be clearly established experimentally[6].

Anticipating that such transient regimes may eventually be measured, we present a few predictions for the optical properties of uniaxially-compressed LiF. Though the strains we consider correspond to stresses well beyond the HEL of LiF, and though our many-body Green's function calculations once again assume perfect crystallinity, we direct our attention to the major differences between hydrostatic compression, and uniaxial compression along the [100]-direction.

Our DFT calculations predict that a 21% compression along the z-direction and a simultaneous 9% expansion along x, y-directions yields a stress tensor which is everywhere zero, save the zz component which has a value of 1 Mbar. Fig. 7a shows the DFT bandstructure of LiF strained in this manner. We note that the uniaxial strain partially removes the 3-fold band degeneracy near the valence band minimum at the Γ-point. Unlike in the case of hydrostatic compression, the minimum band gap at 1 Mbar is at the Γ-point, and is about 0.34 eV *smaller* than the value at P=0. Upon inclusion of electron self-energy corrections at the G_0W_0 level, the bandgap becomes 14.92 eV, *i.e.* 0.58 eV smaller than the predicted quasiparticle gap in ambient (unstrained) conditions. This opposite behavior in the change of the gap with pressure when comparing hydrostatic and uniaxial strains is not unique to LiF; diamond has also been predicted to behave in this way[33].

In fig. 7b we compare the optical spectra of uniaxially-strained and unstrained systems, calculated within the Bethe-Salpeter method. Under uniaxial strain, the optical absorption edge decreases, but its value acquires a

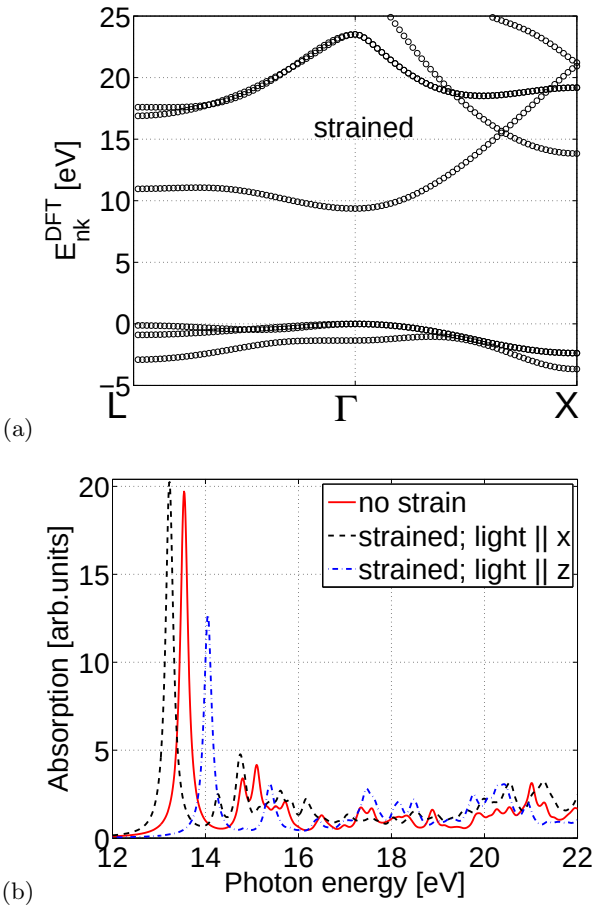

FIG. 7: (a) Electron band structure of uniaxially-strained LiF. We continue to use the X [0 0 1/2] and L [0 1/2 1/2] notations, even though our crystal is no longer cubic, in order to connect to the corresponding **k**-points in the reciprocal lattice of the cubic structure referred to elsewhere here. (b) Optical absorption spectra of uniaxially-strained LiF (for two different light polarizations) compared to the unstrained case.

dependence on the direction of light polarization: i) For polarization perpendicular to z, the absorbtion edge is about 0.31 eV smaller than in the unstrained case; here, the lowest energy bright exciton has a contribution from optically allowed transitions near the Γ point (which originate from the higher energy, doubly-degenerate valence band -see fig. 7a). ii) For polarization parallel to z, the optical absorption edge is higher by roughly 0.5 eV than in the unstrained case; here, the lowest optically allowed transitions take place in a k-space region shifted away from the Γ-point (optically allowed transitions at Γ originate from the lower energy, non-degenerate valence band -see fig. 7a). The effect of these changes on the predicted index of refraction of LiF are notable: The $\perp$ **z** polarization yields an index which is $\sim 1\%$ larger than the unstrained ($P = 0$) value, while the $||$**z** polarization yields an index which is $\sim 2\%$ smaller than the unstrained value.

It is important to note that other choices for the strain state of crystalline LiF may be of interest as well, such as that of keeping the lattice constants in the x and y directions the same as those in the unstrained case, even as a large uniaxial strain is applied to the z axis. This state may indeed be experienced by LiF at the very earliest stages of dynamic compression.

D. Phase-dependent optical properties: B_1 vs. B_2

In addition to variations in the precise state of strain while still in the ambient-phase B_1 (NaCl-type) crystal structure, dynamic compression can also result in principle in LiF changing its crystalline phase. In a recent theoretical work[18], Smirnov predicted the appearance of the B_2 phase (CsCl-type) in the equilibrium phase diagram of LiF above $P \sim 1$ Mbar and $T \sim 3000$ K. Using his multiphase equation of state model fit to *ab initio* electronic structure calculations, he predicted the principal Hugoniot of LiF to pass very close to the $B_1 - B_2 -$ liquid triple-point, and suggested the possibility that some possible final states of single-shock experiments might reside in the field of stability of the B_2 phase. While ramp experiments performed on LiF are far less likely to touch the B_2 phase due to their (assumed) lower temperatures, we nonetheless consider it important to predict the optical properties of LiF in this phase as well, to assess the extent to which a transition from $B_1 \rightarrow B_2$ could substantively alter, for instance, the index of refraction of this window material.

In fig. 8 we compare the calculated absorption spectra (including excitonic effects) of B_1 and B_2 phases, at P= 1 and 2 Mbar. Hydrostatic strain is assumed. As we found for the B_1 phase, the B_2 phase also shows an increase in the optical gap with increasing P, though the magnitude of the gap is ~ 1 eV less than that of B_1 at the same pressures. The main qualitative difference in the predicted absorption spectra in the neighborhood of the absorption edges is the appearance of two large peaks in the B_2 phase, on either side of the single large peak in the corresponding B_1-phase spectra. These differences lead to subtle changes in the refractive index for photon energies well below the optical gap; fig. 9 shows a $\sim 1 - 2\%$ increase in n when going from B_1 to B_2 at the identical conditions, throughout a broad range of photon energies.

IV. CONCLUSIONS

In conclusion, we have presented *ab initio* many-body calculations, including quasiparticle self-energy and excitonic effects, of the electronic and optical properties of LiF at high pressures. We have predicted that the optical absorption spectrum should present dramatic P-dependent features well above the absorption edge, with both quasiparticle and optical gaps increas-

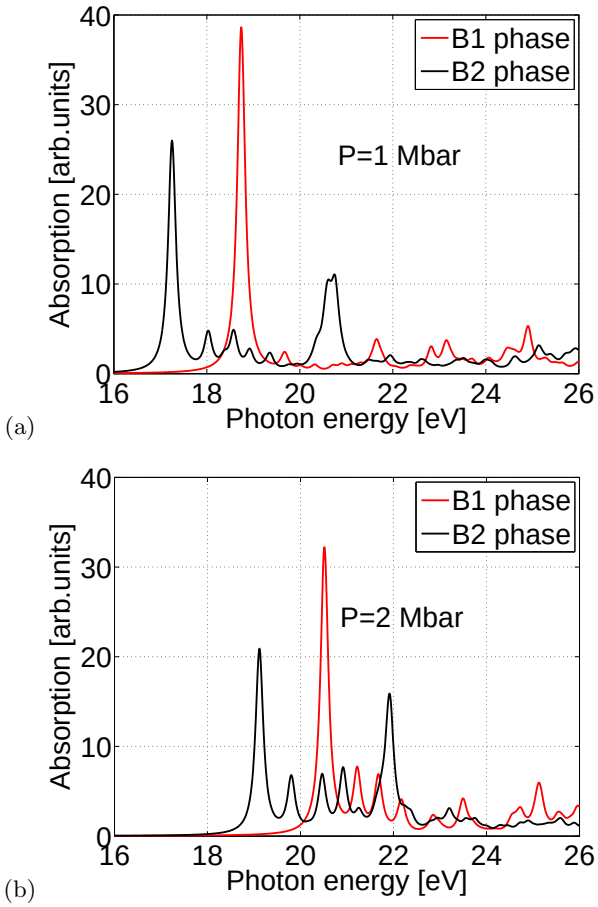

FIG. 8: Optical absorption spectra of B_1 and B_2 phases of LiF at two hydrostatic pressures: (a) $P = 1$ Mbar. (b) $P = 2$ Mbar.

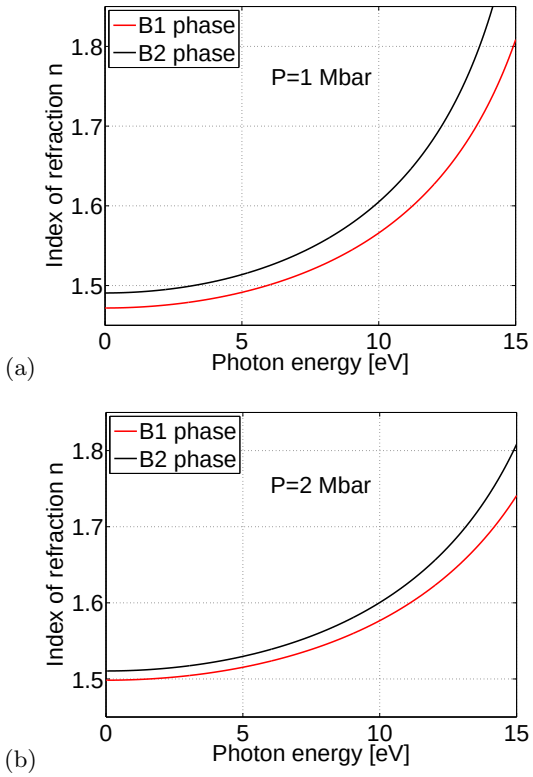

FIG. 9: Index of refraction of LiF as function of photon energy for B_1 and B_2 phases at two hydrostatic pressures: (a) $P = 1$ Mbar. (b) $P = 2$ Mbar.

ing with increasing hydrostatic stress. A marked increase in the magnitude of the near-edge absorption leads to the increase in the long-wavelength index of refraction with increasing P, as measured in numerous recent experiments[5,6,8–11]. This trend compares well with DFT calculations which invoke an independent-particle picture[13], even though the predicted absorption spectra in independent-particle vs. many-body pictures is so radically different. Our prediction of the effect of uniaxial distortion on the optical properties of crystalline LiF reveals polarization dependence as expected in such situations. Finally, we compared our predicted optical properties in the B_1 and B_2 phases, and found that they should have similar indices of refraction for visible and infrared light.

These findings form the basis for future studies of many-electron effects on the optical properties of LiF in states possibly accessed in dynamic compression experiments, where LiF is often used as a window material. In such future studies of the solid, it will be important to consider the role of defects, dislocations, twinning, etc., some subset of which must necessarily be present when a hydrostatic state is reached by applying uniaxial strain beyond the elastic-plastic limit[6]. It is likely the case that these features, along with details of the liquid state, must be modeled accurately to obtain a comprehensive microscopic understanding of the detailed loss of transmission of LiF upon the application of suitably strong shocks[11] and ramps[10].

V. ACKNOWLEDGEMENTS

We thank R.E. Rudd, D.E. Fratanduono, M. Millo, N.C. Holmes, B. Sadigh, and J.H. Eggert for helpful discussions. This work was supported by the ASC/PEM program at SNL. SNL is a multi-program laboratory operated by Sandia Corporation, a Lockheed Martin Co., for the U.S. DOE under contract DE-AC04-94AL85000. Work at LLNL was performed under the auspices of the U.S. DOE under Contract No. DE-AC52-07NA27344.

[1] D.M. Roessler and W.C. Walker, J. Opt. Soc. Am. **57**, 835 (1967).

[2] L.X. Benedict, R.B. Bohn, and E.L. Shirley, Phys. Rev. Lett. **80**, 4514 (1998); M. Rohlfing and S.G. Louie, Phys. Rev. Lett. **81**, 2312 (1998).

[3] For just one of *many* examples in which LiF is used as a window material, see R.F. Smith, J.H. Eggert, A. Jankowski, P.M. Celliers, J. Edwards, Y.M. Gupta, J.R. Asay, and G.W. Collins, Phys. Rev. Lett **37**, 065701 (2007).

[4] In this work, LiF is used in combination with sapphire, another oft-used window material: M.D. Knudson, D.L. Hanson, J.E. Bailey, C.A. Hall, J.R. Asay, and C. Deeney, Phys. Rev. B **69**, 144209 (2004).

[5] J.L. Wise and L.C. Chhabildas, Sandia National Laboratory, Albuquerque, NM, Report SAND-85-0310C, NTIS Order No. DE85015505, 1985.

[6] P.A. Rigg and Y.M. Gupta, Appl. Phys. Lett. **73**, 1655 (1998).

[7] D.G. Hicks, P.M. Celliers, G.W. Collins, J.H. Eggert, and S.J. Moon, Phys. Rev. Lett. **91**, 035502 (2003).

[8] B.J. Jensen, D.B. Holtkamp, P.A. Rigg and D.H. Dolan, J. Appl. Phys. **101**, 013523 (2007).

[9] B.M. Lalone, O.V. Fat'yanov, J.R. Asay, and Y.M. Gupta, J. Appl. Phys. **103**, 093505 (2008).

[10] D.E. Fratanduono, T.R. Boehly, M.A. Barrios, D.D. Meyerhofer, J.H. Eggert. R.F. Smith, D.G. Hicks, P.M. Celliers, D.G. Braun, and G.W. Collins, J. Appl. Phys. 109, 123521 (2011).

[11] P.A. Rigg, M.D. Knudson, R.J. Scharff, and R.S. Hixson, J. Appl. Phys. **116**, 033515 (2014).

[12] S.H. Wemple and M. DiDomenico, Jr., Phys. Rev. B **31**, 1338 (1971).

[13] A. Sajid, G. Murtaza, A.H. Reshak, Mod. Phys. Lett. B 27, 1350061 (2013).

[14] A potential reason for this is that the index of refraction in the long wavelength limit can be obtained from the static dielectric function, which is a ground-state property of the system and is hence well described within the framework of DFT.

[15] J. Clerouin, Y. Laudernet, V. Recoules, and S. Mazevet, Phys. Rev. B **72**, 155122 (2005).

[16] J. Clerouin, Y. Laudernet, V. Recoules, and S. Mazevet, J. Phys. A: Math. Gen. **39**, 4387 (2006).

[17] M.S. Hybertsen and S.G. Louie, Phys. Rev. B **34**, 5390 (1986).

[18] N.A. Smirnov, Phys. Rev. B 83, 014109 (2011).

[19] J. Deslippe, G. Samsonidze, D.A. Strubbe, M. Jain, M.L. Cohen, S.G. Louie, Comp. Phys. Comm. **183**, 12692012 (2012).

[20] W.G. Aulbur, L. Jonsson, and J.W. Wilkins, Sol. St. Phys. **54**, 1 (2000).

[21] L.X. Benedict, C.D. Spataru, and S.G. Louie, Phys. Rev. B **66**, 085116 (2002).

[22] C.D. Spataru, L.X. Benedict, and S.G. Louie, Phys. Rev. B **69**, 205204 (2004).

[23] M. Rohlfing and S.G. Louie, Phys. Rev. B **62**, 4927 (2000).

[24] W. Kohn and L.J. Sham, Phys. Rev. bf 140, A1133 (1965).

[25] A.M. Rappe, K.M. Rabe, E. Kaxiras, and J.D. Joannopolous, Phys. Rev. B **41**, 1227 (1990); N.J. Ramer and A.M. Rappe, Phys. Rev. B **59**, 12471 (1999).

[26] P. Giannozzi et al., J.Phys.:Condens.Matter 21, 395502 (2009).

[27] This cutoff can be far lower than that used to converge the charge density in the DFT calculation. The lower energy cutoff requirements for W_0 are described, for instance, in M. Rohlfing and S.G. Louie, Phys. Rev. B **62**, 4927 (2000).

[28] G. Onida, L. Reining, and A. Rubio, Rev. Mod. Phys. **74**, 601 (2002).

[29] A. A. Mostofi, J. R. Yates, Y.-S. Lee, I. Souza, D. Vanderbilt and N. Marzari, Comput. Phys. Commun. **178**, 685 (2008).

[30] At ambient pressure, LDA underestimates the equilibrium lattice constant of LiF by $\sim 3\%$. We find that the LDA band gap increases by 0.9 eV when the experimental lattice constant is used (with respect to the case where the theoretical lattice constant is employed). This explains why our calculated optical gap at ambient pressure is slightly larger than both the experimental gap and the gap found in other *ab initio* studies[2].

[31] In addition, a collection of quasiparticle gap energies for LiF, both computed and measured, appears in Table I of E.L. Shirley, L.J. Terminello, J.E. Klepeis, and F.J. Himpsel, Phys. Rev. B **53**, 10296 (1996).

[32] D. Pan, Q. Wan, and G. Galli, Nat. Comm. **5**, 3919 (2014).

[33] M.P. Surh, S.G. Louie, and M.L. Cohen, Phys. Rev. B **45**, 8239 (1992).